Behavior of RC Columns Confined with CFRP Sheets and Subjected to Eccentric Loading

Omar A. Farghal[1]and Mamdouh A. Kenawi[2]

[1]Civil Engineering Department, Faculty of Engineering, Assiut University, Egypt.
[2]Civil Engineering Department, Faculty of Engineering, Sohag University, Egypt.

e-mail: omar_farghal222@yahoo.com; mkenawi2@yahoo.com

Abstract: Reinforced concrete (RC) rectangular columns with aspect ratio of approximately 1.5 and externally confined with bonded carbon fiber reinforced polymers (CFRP) sheets were experimentally subjected to eccentric compression loads up to failure. The effect of the value of eccentricity and confinement configuration (fully confined (*FC*) and partially confined (*PC*)) on the behavior of the strengthened columns was studied. The experimental results showed that both strength and ductility of the strengthened columns had been improved with respect to the behavior of the reference columns. The improvement in column compressive strength of both FRP-confinement systems applied under eccentric loading was so pronounced as for that under concentric loading. Furthermore, an analytical study was conducted aiming to apply models proposed by the ACI guidelines for strengthening concrete structures with FRP (ACI 440.2R-02 and ACI 440.2R-08) to evaluate the enhancement of the strengthened columns. To overcome the well-defined weaknesses of applying these models, a simplified analytical form is proposed to assess the enhancement in column strength under the effect of eccentric loading. The proposed analytical model showed an agreement with the constructed theoretical axial force-moment (P-M) interaction diagram for FRP-confined concrete using ACI 440.2R-08. Ultimately, the proposed model provides a reasonable approach for evaluating the increase in the strength of eccentrically loaded fully or partially confined RC columns.

[Omar A. Farghaland Mamdouh A. Kenawi**. Behavior of RC Columns Confined with CFRP Sheets and Subjected to Eccentric Loading.** *Life Sci J* 2018;15(6):22-39]. ISSN: 1097-8135 (Print) /ISSN: 2372-613X (Online).http://www.lifesciencesite.com. 4. doi:10.7537/marslsj150618.04.

Keywords:FRP sheets; Wrapping; Rectangular; P-M; Eccentricity; Confinement.

1.Introduction

Confinement of reinforced concrete columns by means of FRP jackets is commonly used to enhance their strength and ductility. An increase in capacity is an immediate outcome typically expressed in terms of improved peak load resistance. Concrete columns have important function in the structural concept of structures. Often these columns are vulnerable to load increase (change of structures' function, etc.), exceptional loads (such as: impact; explosion or seismic loads) and degradation (corrosion of steel reinforcement, alkali silica reaction, etc.).

In practice, structural concrete columns axially compressed (i.e., concentrically) rarely occur. Even in a column nominally carrying only axial compression, bending action is almost always present due to unintentional load eccentricities and/or possible construction error. However, research studies conducted so far on external confinement of concrete columns have mainly concentrated (focused) on concentric loading [1- 8]. Few researches are known about the behavior of strengthened RC columns subjected to eccentric loads [9 - 14].

Previous research studies showed that, when confined columns are subjected to axial loading, FRP composites could provide adequate lateral stresses. However, under eccentric loading, some researches confirm that no significant effect is achieved, while others attested that confining columns with FRP composites can improve the structural performance to some extent. Since the problem is quite complicated, very few stress–strain models have considered load eccentricity. In fact, some results contradict others. El Maaddawy[15] suggested that the stress–strain curve for concentrically loaded columns may be used for eccentrically loaded columns also, except that the final point (ultimate failure point) of the stress–strain curve.

This study presents experimental and analytical evaluation of the effectiveness of fiber reinforced polymers (FRP) composites to strengthen RC columns subjected to eccentric loading. The experimental program included eight rectangular RC columns tested under compression load with eccentric ratios (e/h = 0.0, 0.13, and 0.17). Three samples were fully confined (*FC*) with one layer of CFRP sheet, two samples were partially confined (*PC*) with two layers of CFRP sheet, and three columns served as references. To analytically evaluate the strength enhancement of FRP-confined RC columns, proposed models by ACI guidelines for strengthening concrete structures with FRPs (ACI 440.2R-02 [16] and ACI 440.2R-08 [17]) were examined. Moreover, a simple model based on linear and nonlinear geometrical properties of the transformed cross-section was

proposed and evaluated in the light of both the available test results and the constructed P-M diagram using the stress-strain model of FRP-confined concrete adopted by ACI 440.2R-08 [17]. The obtained results concerning the maximum loads were also employed to study the applicability of the analytical model suggested by the authors to predict the nominal compressive strength of RC columns fully or partially confined with CFRP sheets and subjected to eccentric loads.

2. Experimental Studies

2.1. Layout of Experiments and Materials

The experimental program includes eight RC rectangular columns and tested under eccentric loading, see Table 1. The cross-section of the tested columns has a dimension of 160 x 250 mm ($b \times h$) and the total height of column's specimens is 960 mm. These columns were reinforced with six high strength deformed bars, 6 Φ12 mm, (Steel 360/520 having proof stress, tensile strength, and Young's modulus of 386, 578, and 216000 MPa). These columns were provided with internal closed stirrups (Steel 240/350 where their yield and tensile strengths are 280 and 410MPa) of 6mm in diameter and 125mm spacing (S). It is worth mentioning that each end zone of all studied columns was reinforced with 5 steel stirrups of 6mm in diameter (steel 240/350), as shown in Fig. 1 and Table 1. The mean compressive strengths for the standard cylinder ($f_c^{/}$) and cube (f_c) after 28 days for all tested columns were listed in Table 1. The wrapping reinforcement was a CFRP sheet of 0.16 mm effective fiber thickness (t_f). The tensile strength, maximum strain, and E-modulus of such CFRP sheet are (according to the manufacturer) 3550 N/mm^2, 1.5%, and 230000MPa, respectively. The resin used to impregnate the CFRP sheets is a special one having tensile strength and flexural E-modulus (in accordance with the manufacturer) of 30 and 3800MPa, respectively.

The designation of the tested columns *R*, *FC*, and *PC* indicate the reference, fully-confined and partially-confined, respectively, and0,13,17 denote the eccentricity ratio to the column depth (*e/h = 0.0, 0.13*, or *0.17*). Three columns (*R.0, R.13* and *R.17)*were tested without strengthening as control samples. Three columns (*FC.0*, *FC.13* and *FC.17*) were confined with one ply of CFRP sheet applied over the total area in a circumferential way, as shown in Fig. 2. The last two columns *PC.0* and *PC.17*were confined with two plies of CFRP strips each of 65-mm width (b_f) and 65-mm free spacing (S_f). The discontinuous CFRP strips were distributed uniformly along the length (710-mm), as shown in Fig. 2. It isworthwhile to mention that the strengthened columns were confined with the same amount of fiber reinforcement (ρ_f = volume ratio of wrapped CFRP sheet = 3.29 ‰). Moreover, to avoid local failure of the ends of the tested columns, they were confined with two layers of CFRP sheet of 125-mm width, as shown in Fig. 2. The unidirectional CFRP sheets were bonded with a fiber orientation perpendicular to the longitudinal axis of the columns, corresponding to the loading axis. When executing the CFRP wrapping system, an overlap length of 100-mm in the hoop direction was applied for the different columns (no overlap was provided in the longitudinal direction for full wrapping). For the different tested columns, the cross-sectional cornershad been rounded in a curved shape of 50-mm diameterto avoid stress concentration at the corners' zones.

Table 1: Data of tested columns

Column No.	Columns data					Strengthening system
	f_c (MPa)	$f_c^{/}$ (MPa)	A_s	Internal stirrups	Eccentricity (e)	
R.0	26.0	21.0	6 Φ 12 mm	1 φ 6 mm @ 125 mm	e = 0.0 mm (e/h = 0.00)	Control column 1
R.13	26.5	21.5			e = 31.5 mm (e/h = 0.13)	Control column 2
R.17	27.0	22.0			e = 41.5 mm (e/h = 0.17)	Control column 3
PC.0	26.0	21.0			e = 0.0 mm (e/h = 0.00)	Partially confined: 5 strips, each of 65-mm width & 65 mm free spacing (two plies, $\mu_f \approx$ 3.29 ‰)
PC.17	27.0	22.0			e = 41.5 mm (e/h = 0.17)	
FC.0	26.0	21.0			e = 0.0 mm (e/h = 0.00)	Fully confined (one ply, $\mu_f \approx$ 3.29 ‰)
FC.13	26.5	21.5			e = 31.5 mm (e/h = 0.13)	
FC.17	27.0	22.0			e = 41.5 mm (e/h = 0.17)	

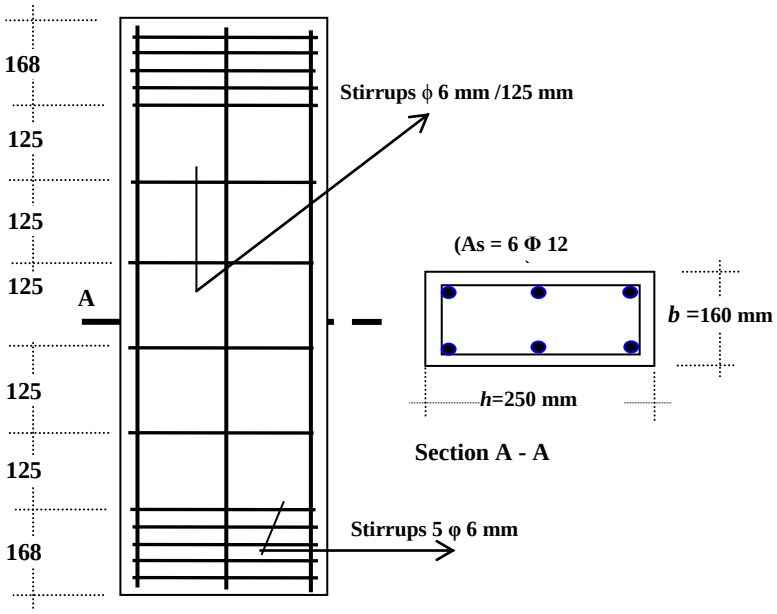

Figure 1. Details of internal reinforcement for tested columns.

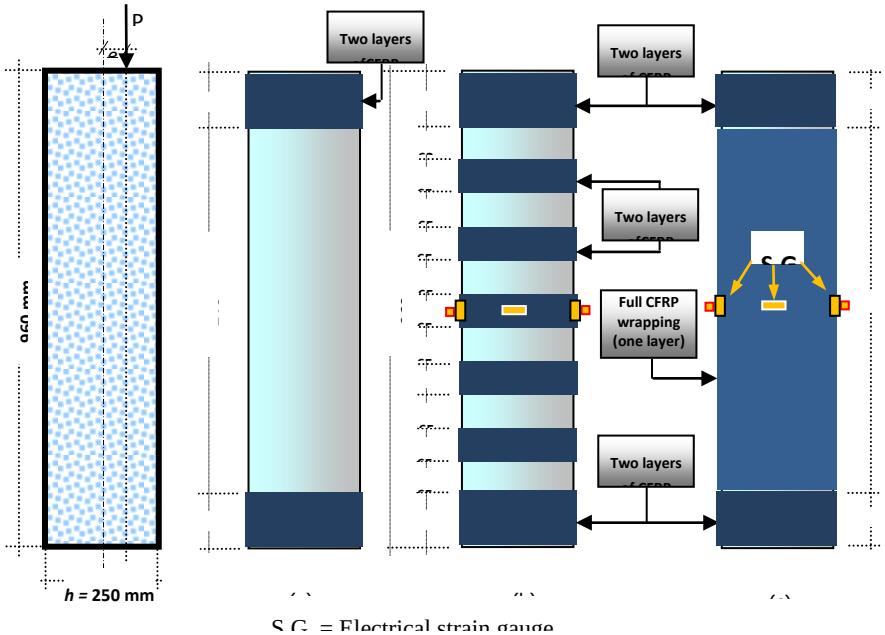

Figure 2. Details and arrangements of bonded CFRP sheets for tested columns:(a) Control ones, (b) Partialconfinement, and (c) Full confinement.

2.2. Instrumentation

The transverse strain induced in FRP sheets were measured using four electrical strain gauges which were affixed on the surface of the fibre sheets at the mid-height, as shown in Fig. 2. Also, the vertical strains induced in the concrete at the mid-height were measured using additional two electrical strain gauges affixed on the fibre sheets for FRP-confined columns and onthe surface of concrete in case of the control columns. Moreover, to measure the vertical shortening occurred in all tested samples, an LVDT (linear variable displacement transducer) was used.To record the different measurements regularly every optional interval (1 second), both the LVDT and strain gauges

were connected with data acquisition system (TDS-150) which in turn was connected with a computer.

3. Experimental Results and Discussion

A summary of the observed results of all tested columns is presented in Table 2, which includes: cracking load P_{cr}; maximum load(P_{max}); ratio of maximum load of the FRP-confined column to their corresponding control column (R); maximum mean normal stress ($\sigma_{c,max} = P_{max}/A_g$), where A_g is the gross sectional area; mean axial strain induced in the concrete ($\varepsilon_{c,mean}$) corresponding to failure; $\Delta h_y$and $\Delta h_{ymax}$are the total axial shortening in the tested columncorresponding to both yielding and failure, respectively; ductility factor μ_D(= Δh_{ymax} /Δh_y); failure modes of all columns; and transverse (hoop) strains of CFRP sheets (at mid-height) corresponding to failure: ($\varepsilon_{f\text{-}X}$) the average of the two transverse strains measured at the two opposite long directions and ($\varepsilon_{f\text{-}Y1}$&$\varepsilon_{f\text{-}Y2}$) the hoop strains measured at the two opposite short directions subjected to the maximum and minimum normal stresses, respectively.

Table 2: Experimental results for tested columns

Column No.	P_{cr} [kN]	P_{max} [kN]	R [-]	P_{cr}/P_{max} [-]	Max. normal stress & strains		Max. circumferential CFRP strains			Shortening & ductility			Failure mode
					$\sigma_{c,mean}$ [MPa]	$\varepsilon_{c,mean}$ [mm/mm]	$\varepsilon_{f,max\text{-}X}$ [με]	$\varepsilon_{f,max\text{-}Y1}$ [με]	$\varepsilon_{f,min\text{-}Y2}$ [με]	Δh_y [mm]	Δh_{max} [mm]	μ_D [-]	
R.0	1075	1124	1.00	0.957	28.10	0.0037	----	----	----	2.51	3.89	1.55	F.M.1
R.13	1014	1061	1.00	0.956	26.53	0.0035	----	----	----	2.28	3.63	1.59	F.M.1
R.17	959	1004	1.00	0.955	25.10	0.0035	----	----	----	2.19	3.50	1.60	F.M.1
PC.0	1240	1331	1.18	0.932	33.28	0.0060	5560	5050	5355	2.52	6.53	2.59	F.M.2
PC.17	980	1118	1.11	0.877	27.95	0.0055	3452	3925	3343	2.19	6.15	2.81	F.M.2
FC.0	1285	1406	1.25	0.914	35.15	0.0062	>9193 [(a)]	8024	9918	2.54	7.01	2.76	F.M.3
FC.13	1099	1260	1.19	0.872	31.50	0.0057	4571	5154	4410	2.26	6.14	2.72	F.M.3
FC.17	1000	1218	1.21	0.821	30.45	0.0060	4119	3938	3287	2.21	6.24	2.84	F.M.3

Note: F.M.1, F.M.2, and F.M.3 are the first, second, and third failure modes, respectively.

(a) One of the two strain gauges located at X-direction teared due sudden rupture of FRP sheet.

3.1. Cracking and Maximum Loads

It is interesting to define the cracking load to enrich the basic knowledge of design engineers with the performance of eccentrically loaded columns confined fully or partially with FRP sheets. Clearly, this will provide information about the end of un-cracked stage. As a consequence, the cracking load for the reference columns corresponded to observed-first-crack on the column surface. For partially confined columns, the load corresponding to the first noticed crack between the FRP strips defines the cracking load. However, for fully confined columns, the cracking load was defined based on a strong "popping" sound accompanied by bends on the bonded fiber sheets. Accordingly, the cracking loads for all tested columns are defined and summarized in Table 2. Through this table, it is obvious that the strengthened columns showed an enhancement in comparison with their corresponding reference columns, particularly in case of *FC*-columns regardless of the value of eccentricity. However, the value of eccentricity affected inversely the cracking load. For instance, in case of concentrically loaded columns (*e/h=0.0*), the cracking load was 1075, 1240, and 1285 kN for *R.0*, *PC.0*, and *FC.0*, respectively; however, for the columns *R.17*, *PC.17*, and *FC.17* subjected to eccentric loading (*e/h = 0.17*), the cracking load was 959, 980, and 1000 kN, respectively, as shown in Fig.3. For maximum load, in general, the eccentricity was responsible for the decrease in the maximum carrying capacity of the tested columns compared with the axially loaded columns. In other words, axially loaded columns showed an improvement in the load carrying capacity higher than that of eccentric loaded columns, as shown in Fig.4. This can be clearly found in the results of fully confined columns, which showed improvement of 25, 19 and 21% when eccentricities were 0.0, 31.5 and 41.5-mm respectively. In addition, for partially confined columns, the improvement was 18 and 11% in case of eccentricities of 0.0 and 30-mm, respectively, as shown in Fig.5. As a consequence,

either in case of fully confined columns or partially confined columns, both cracking and maximum loads as well as strengthening efficiency are inversely proportional to the eccentricity ratio (*e/h*). Moreover, regardless of the value of eccentricity, for the same strengthening degree ($\rho_f \approx 3.29$ ‰), the *FC*-columns showed a higher efficiency than the corresponding *PC*-columns; so fully confined system should be applied when it is possible. This confirms what was verified by Farghal and Diab [18]. They concluded that to enhance the performance of *PC*-columns, spacing between strips of FRP sheets should be minimized to confine the maximum possible area of the column.

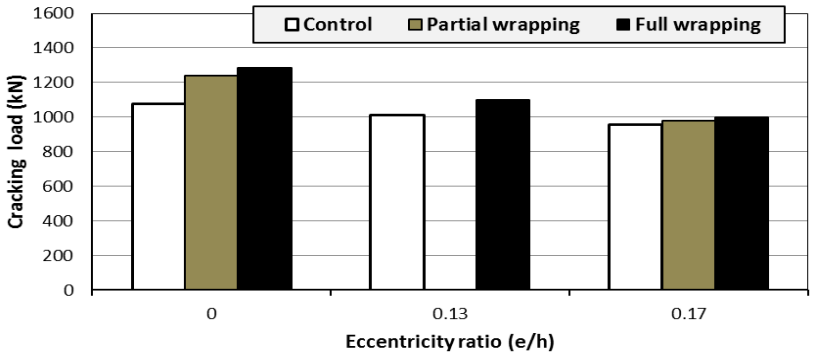

Figure 3. Cracking load (P_{cr}) for the different eccentricity ratios (*e/h*).

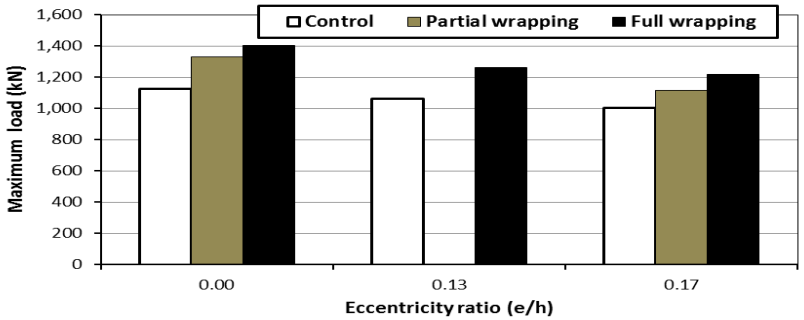

Figure 4. Maximum normal load (P_{max}) for the different eccentricity ratios (*e/h*).

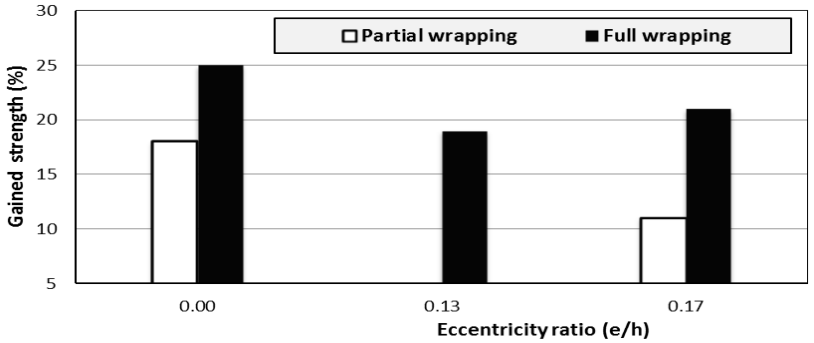

Figure 5. Gain in strength for the different eccentricity ratios (*e/h*).

Table 2 summarizes also the ratio of the cracking load to maximum load (P_{cr}/P_{max}), and it is remarkable that the strengthened columns had the smallest values compared with the reference columns, mainly when load eccentricity increased. That is, the first crack initiated at a load level of about 0.96 times the maximum load in case of the control columns; however, it initiated at a load level smaller than 0.93 times the maximum load in case of strengthened columns depending mainly on the value of the eccentricity and confinement configuration. In case of the control columns, the value of eccentricity showed approximately no clear effect on the ratio of cracking load to maximum load (P_{cr}/P_{max}): the ratio (P_{cr}/P_{max}) equal to 0.957, 0.956 and 0.955 when *e/h* equal to 0.0, 0.13 and 0.17, respectively. However, for the

strengthened columns, the ratio (P_{cr} /P_{max}) decreased as the eccentricity increased for both confinement configurations used. The *PC*-columns showed cracking to maximum load ratios of 0.932, and 0.877 when (*e/h*) equal to 0.0 and 0.17, respectively. Also, the *FC*-columns *FC.0*, *FC.13*, and *FC.17*showedP_{cr}/P_{max} ratios of 0.914, 0.872 and 0.821, respectively, as shown in Fig.6. As a consequence, the ratio of cracking load to maximum load (P_{cr} /P_{max}) is inversely proportional to the eccentricity ratio (*e/h*). This could be attributed to the fact that the failure had not occurred until the confinement allowed the redistribution of normal stress along the entire column cross-section, and at that time rupture of wrapped CFRP sheets took place. As a result, the cracks of concrete propagated in the concrete section more than the control ones in which the failure occurred when the crushing of concrete initiated in the extreme fibers of the section. This is clearly observed from bends of the wrapped sheet occurred not only across the cross-section but also along the height of the columns.

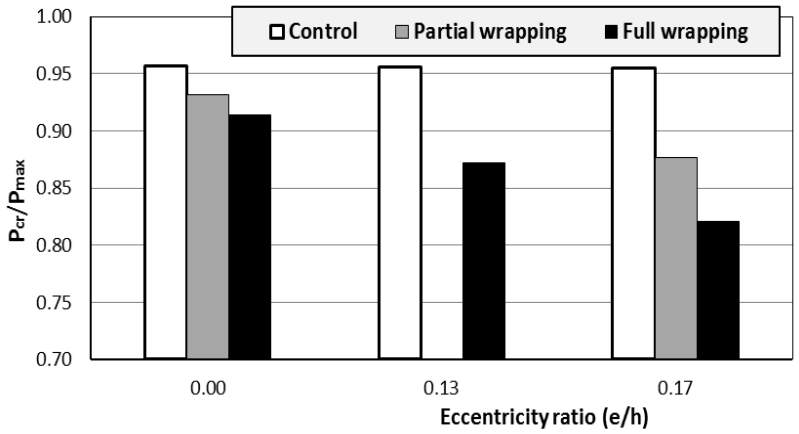

Figure 6. Cracking load to maximum load ratio (P_{cr} /P_{max}) for the different eccentricity ratios (*e/h*).

3.2. Failure Mode

Three mechanisms of failure were observed throughout the experimental tests carried out on FRP-confined and un-strengthened rectangular RC columns. The first mechanism was due to crushing of concrete formed along the height of the columns. The second mechanism was also due to crushing of concrete which was seized at the unconfined zones between CFRP strips. The third mechanism was due to rupture of CFRP sheet.

The first failure mechanism occurred for both concentrically and eccentrically loaded columns (*R.0*, *R.13*, and *R.17*), as shown inFig.7(a). For the control column *R.0* subjected to axial load (*e/h* = 0.0), the crushing of concrete was due to somewhat an inclined crack initiated at the upper third zone and propagated suddenly causing failure accompanied with a crushing of the concrete cover at that zone, as shown in Fig.7(a). For control columns *R.13* and *R.17* subjected to eccentric loads (*e/h* = 0.13 and 0.17, respectively), the crushing of concrete was for the concrete cover at the column zone of the highest compressive stresses (towards the side of higher compressive stress where the load was applied), as shown inFig.7 (a).

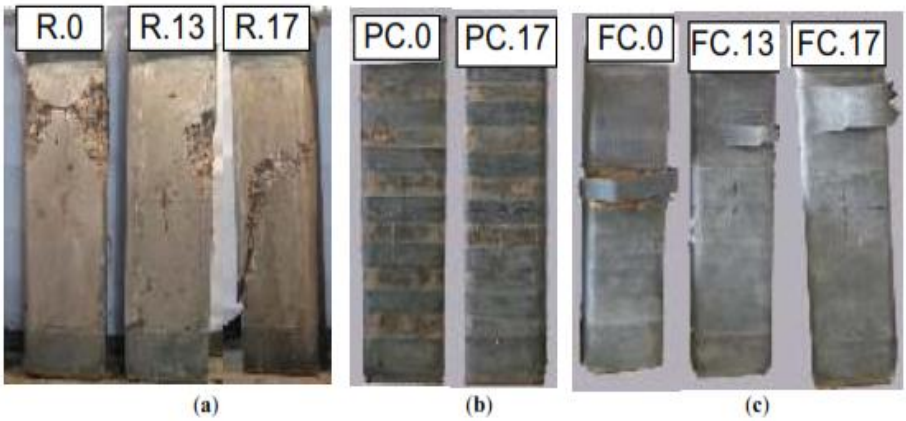

Figure 7. Failure aspect of different columns:(a) Control *R.*-(b) Partially confined*PC.*, and(c) Fully confined*FC.*

The second failure mechanism was observed for *PC*-columns subjected to either concentric or eccentric loading *PC.0* and *PC.17* (*e/h* = 0.00 and 0.17). These columns realized concrete crushing formed at the unconfined zones between CFRP strips, as shown inFig.7(b). The concrete crushing in case of the *PC.0* column was formed in the middle third zone through approximately the whole cross-section; however, for *PC.17* it was formed in the upper third and located in side where the load was applied, as shown in Fig.7 (b).

The third failure mechanism was due to rupture of CFRP sheet and occurred for the fully FRP-confined columns (*FC.0, FC.13 and FC.17*). When the load applied was concentric, (the columns *FC.0* (*e/h* = 0.0), the failure was due to cut-offof the fiber sheet bonded at the middle third of the column's height accompanied with a delamination of concrete cover along approximately the whole perimeter of the cross-section, as shown in Fig.7(c). However, for the *FC*-columns subjected to eccentric loading (*e/h* = 0.13 and 0.17),the failure detected was due to rupture of CFRP sheet located at the top third of the column's height accompanied with both a partial delamination of concrete cover and local concrete crushing, as shown in Fig.7(c). It is obvious that the concrete crushing located at the concrete zones of higher compressive stress close to the part of cross-section where the load was applied. It is worthwhile to mention that the rupture of CFRP sheet initiated at the long side of the cross-section (x-direction) in case of columns subjected to axially load (*e/h* = 0.0), however for the columns subjected to eccentric load (*e/h* = 0.13 and 0.17) the rupture of CFRP sheet initiated at the short side of the cross-section (y-direction): the side exposed to the maximum compressive stresses.

3.3. Stress-Strain Behavior

3.3.1.Mean compressive stress-mean concrete strain relation

The affixed vertical strain gauges to column surface at its mid-height cannot accurately represent the behaviour of the entire column, so the measured axial concrete shortening was used to determine the mean axial strain (= axial shortening/column height) and plotted in Figs. 8 and 9 versus the nominal compressive stress level (P / A_g) for all tested columns. In these figures, the FRP-confined columns displayed somewhat linear stress-strain relationship up to the cracking load level, which was then followed by a nonlinear behavior. No warning was observed before failure in case of the un-strengthened columns. However, in case of the FRP-confined columns, a reasonable ductility was noticed before failure, as shown in Figs. 8 and 9. The FRP-wrapping technique also showed a reasonable effect on the axial stiffnesses of the columns, particularly after cracking. The fully confinement technique was able to decrease the column deformation in the longitudinal axis (shortening) showing the highest stiffness compared with both *PC*-columns and un-strengthened samples, as shown in Figs. 8 and 9. Effects of load eccentricity on mean compressive stress-strain relation were insignificant up to the cracking level; however, after exceeding the cracking load, the increase in load eccentricity was associated with a considerable increase in column shortening which inversely affected its stiffness.

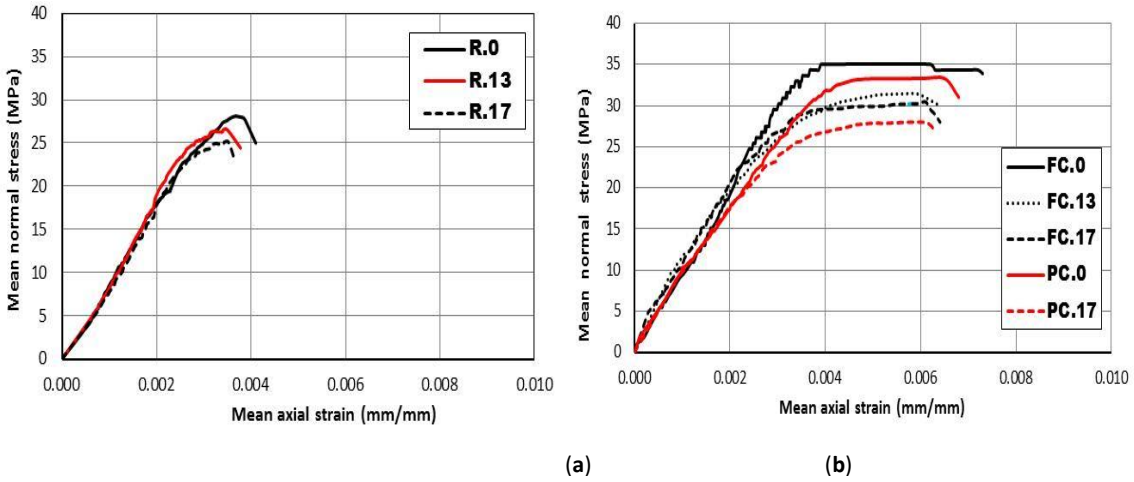

Figure 8. Mean normal stress-axial strain diagrams for tested columns: (a) Control column *R.-*, and (b) Confined column*PC.-*&*FC.-*.

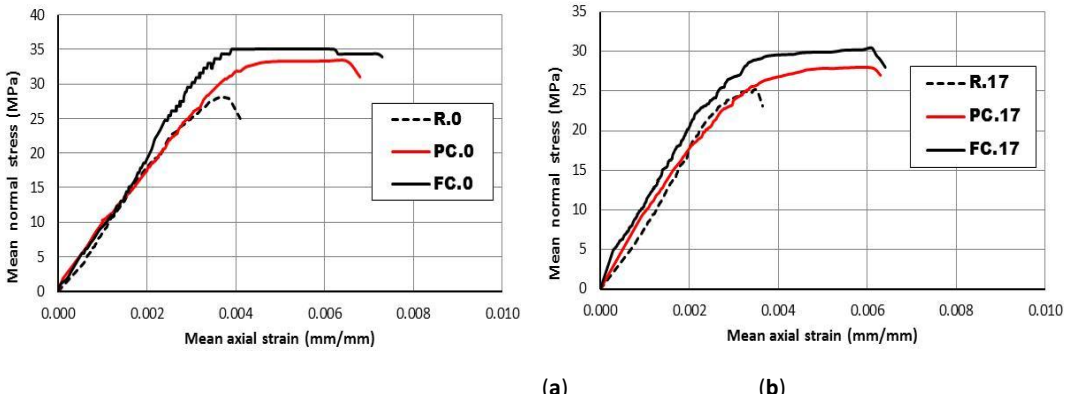

Figure 9. Mean normal stress-axial strain diagrams for tested columns:(a) Concentric loaded, and (b) Concentric loaded.

3.3.2.Mean compressive stress-CFRPcircumferentialstrainrelation

The axial stress-CFRP transverse strain behavior for the confined columns is shown in Fig. 10. The CFRP transverse strain was recorded at the mid height for different directions: ($\varepsilon_{f\text{-}X}$) the average of the two transverse strains measured at the two opposite long directions and ($\varepsilon_{f\text{-}Y1}$&$\varepsilon_{f\text{-}Y2}$) the transversestrains measured at the two opposite short directions exposed to the maximum and minimum stresses, respectively.

Throughout the nominal compressive stress-CFRP hoop strain behavior of the tested confined columns (Fig. 10), it is obvious that the normal stress-CFRP strain relation for the different measured strains ($\varepsilon_{f\text{-}X}$, $\varepsilon_{f\text{-}Y1}$&$\varepsilon_{f\text{-}Y2}$) was approximately linear up to a certain normal stress level, which was dependent on the value of eccentricity. Such normal stress was approximately 25, 18 and 15 MPafor *FC-* columns of eccentricity ratio (*e/h*) of 0.0, 0.13 and 0.17, respectively. However, for *PC-* columns such stress level has no obvious relation. Afterwards, once the columns are loaded beyond this stress level, a nonlinear relation was noticed. When considering the CFRP strain corresponding to the failure, for confined columns (*PC.0*&*FC.0*) axially loaded (*e/h = 0.0*) the CFRP strain $\varepsilon_{f\text{-}X}$ was higher than $\varepsilon_{f\text{-}Y1}$ and $\varepsilon_{f\text{-}Y2}$. On the other side, as the eccentricity increased $\varepsilon_{f\text{-}Y1}$ increased and both $\varepsilon_{f\text{-}Y2}$ and $\varepsilon_{f\text{-}X}$ decreased. In the light of this, it is clear that the reason phenomena of the position of rupture initiation of CFRP sheet: the rupture initiated at the long direction (x-direction) for column *FC.0*, however it initiated at the short direction (y-direction) for column *FC.17*. This is attributed to the fact that, the rupture of the bonded CFRP sheet occurred at the concrete zone in which the higher CFRP strain induced. For instance, in case of column *FC.0* the rupture of CFRP initiated along the length of cross-section (x-direction) of higher CFRP horizontal strain: $\varepsilon_{f\text{-}X}$, $\varepsilon_{f\text{-}Y1}$ and $\varepsilon_{f\text{-}Y2}$ were > 9193 (one of the two strain

gauges located at X-direction (long side) teared due sudden rupture of FRP sheet), 8024 and 9918 micro-strain ($\mu\varepsilon$), respectively. However, in case of column *FC.17* the rupture of CFRP initiated along the width of cross-section (y1-direction of maximum normal stress): $\varepsilon_{f\text{-}X}$, $\varepsilon_{f\text{-}Y1}$ and $\varepsilon_{f\text{-}Y2}$ at mid-height were 4119, 3938 and 3287$\mu\varepsilon$, respectively. It is interesting to mention that in case of column *FC.13* ($\varepsilon_{f\text{-}X}$, $\varepsilon_{f\text{-}Y1}$ and $\varepsilon_{f\text{-}Y2}$ were 4571,5154 and 4410$\mu\varepsilon$, respectively) the CFRP strains induced in both directions "X&Y1" were somewhat close each other (4571 and5154$\mu\varepsilon$). So the rupture of CFRP initiated along the corner of cross-section close considerably to tangency of the corner with length of cross-section (between X-and Y1-directions).

Through Fig.10 and Table 2, it is obvious that the *FC*-columns failed due to the rupture of the CFRP sheet showed a higher maximum hoop strain compared with those partially confined *PC*, which failed due to concrete crushing at the free zones (unconfined zones). The values of hoop CFRP strain give an indication about the degree of taking advantage of the applied confinement technique. Hence, the efficiency of the applied strengthening technique is expressed by the ratio of the induced circumferential CFRP strain to the ultimate strain of the used CFRP sheets. As a consequence, the *FC*-columns satisfied higher strengthening efficiency in comparison with the *PC*-columns. Moreover, it is important to mention that, although a rupture of CFRP strips has occurred in case of *FC*-columns, the induced maximum CFRP strain had not reached the expected ultimate value of the CFRP strain (about 15000 $\mu\varepsilon$). This is attributed to the fact that the cut-off of CFRP jacket had not exactly occurred where the strain gauges used were installed.

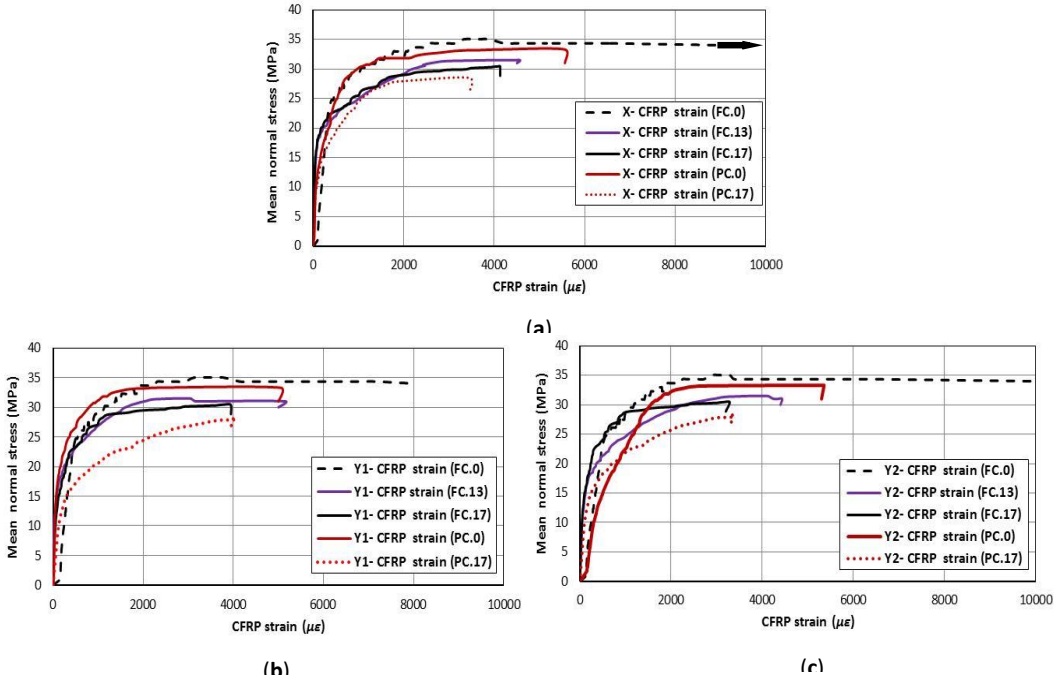

Figure 10. Mean normal stress-circumferential CFRP strain diagrams for confined columns: (a) X-direction, (b)Y1-direction&(c) Y2- direction.

3.4. Structural Ductility

For any structural design, ductility is a required feature as an extra safety factor against unexpected overloading. Generally, for a structural member subjected to axial load, ductility may be measured by the ductility factor (μ_D) which is equal to the total axial shortening at ultimate load or failure (Δh_{max}) to that at the beginning of yielding of main steel reinforcement (Δh_y). The total axial shortening generated in the structural member at failure (Δh_{max}) is defined as the shortening occurred in the member at failure, e.g. cut-off of FRP sheets or crushing of concrete or when strength descends to 85 % of the maximum load. Careful scrutiny of the test results showed that the total vertical shortening corresponding to the first yielding of internal main reinforcement (Δh_y) decreased as the eccentricity increased without any clear effect for the type of confinement configuration (*PC* or *FC*) on Δh_y. For instance, the shortening corresponding to the first yielding was more or less 2.50, 2.30 and 2.20 mm for eccentricities of 0.0, 31.5 and 41.5 mm, respectively. This can be attributed to the local effect of the eccentric loading which caused a significant increase

in the compressive stresses and strains in steel reinforcement as the eccentricity increased.

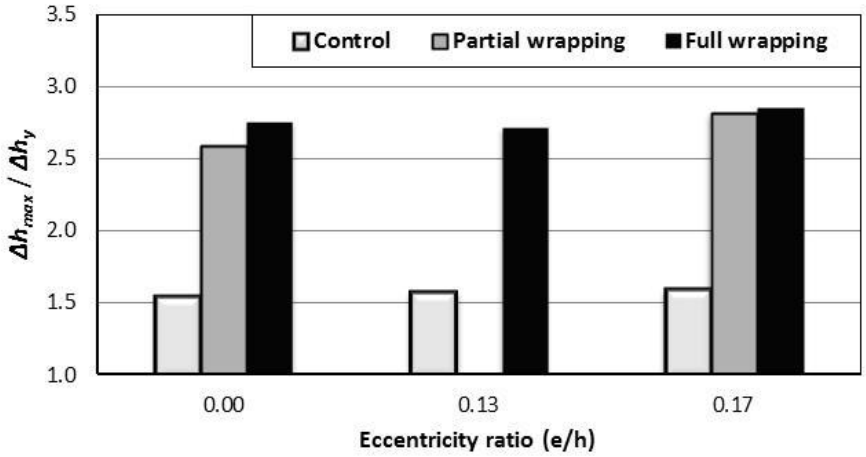

Figure 11. Ductility index μ_D (= Δh_{max} /Δh_y) for the different eccentricity ratios (*e/h*).

From the view point of the required gradual degradation of column strength after achieving the maximum capacity, it is obvious that FRP-confinedcolumns showed a reasonable deformation after reaching the maximum load, but control columns failed without sufficient warning approximately at the maximum load level. It is worthwhile to note that, when compared with the control columns, the FRP-confined columns showed a considerable enhancement in the obtained ductility μ_D (= Δh_{max} /Δh_y), especially in case of *FC*- columns, as shown in Fig.11 and Table 2. For instance, in case of axial loading, the ductility index was 1.55, 2.59 and 2.76 for control, *PC*- and *FC*- columns. Also, for eccentric loading (*e/h* = 0.17), the ductility index μ_D was 1.60, 2.81 and 2.84 for control, *PC*- and *FC*-columns respectively. It is worth to note that, in case of control- and *FC*-columns, eccentricity has no obvious effect on the obtained ductility: the fully confined column *FC.0*, *FC.13*, and *FC.17* had ductility indices of 2.76, 2.72 and 2.84, respectively; and un-strengthened columns *R.0*, *R.13*, and *R.17*, showed ductility indices of 1.55, 1.59 and 1.60, respectively. However, in case of*PC*-columns, eccentricity showed a reasonable effect on the obtained structural ductility: the ductility indices for the partially confined columns *PC.0* and *PC.17* were 2.59 and 2.81, respectively, see Table 2.

4. Analytical Modeling

Confining RC columns with FRP sheets leads to improve the strength of concrete; namely confined concrete strength f'_{cc} . As a consequence, the compressive strength of the concrete column is improved. The degree of confinement in terms of the amount of wrapping FRP influences considerably the confined concrete strength f'_{cc} . So, the compressive strength of non-slender RC FRP-confinedcolumns P_{max}may be predicted in a similar way as that of un-strengthened RC members, using confined concrete strength f'_{cc} according to Eq. (1).

$$P_{\max} = k_c\, f'_{cc}\,(A_g - A_s) + f_s\, A_s \qquad (1)$$

where A_g is the gross area of concrete section, A_s is the total area of main reinforcement, f'_{cc} is the confined concrete compressive strength based on cylinder, k_c is a factorwhich takes into account the size effect (k_c =0.85) and f_s is the stress generated in the main steel reinforcement at a load level equals the maximum load of the FRP-confinedcolumn P_{max}.

The following section presents a summary of the models proposed by the ACI 440.2R-02 [16] and ACI 440.2R-08 [17] to predict the compressive strength of RC columns confined with FRP jackets. After that, in the light of the study conducted on these models, a simplified analytical form is proposed to evaluate the enhancement in the column capacity under the action of small eccentricity ($e < h/6$) after strengthening with external FRP jacket using full or partial wrapping configurations.

4.1. Prediction of Nominal Compressive Strength ofFRP-Confined RC Columns under Eccentric Loading Using ACI 440.2R-02 & ACI 440.2R-08.

ACI 440.2R-02 [16] provided an analytical form to predict the axial compressive strength of a nonslender, normal weight concrete member confined with an FRP jacket and with existing steel longitudinal reinforcement, Eq. (2).

$$P_n = 0.85\,\psi_f\, f'_{cc}\,(A_g - A_s) + f_y\, A_s \ \{\text{ACI440.2R-02}\} \qquad (2)$$

Where f_y is the yield strength of the main steel reinforcement and ψ_f is a factor equal to 0.95.

ACI 440.2R-02 [16] adopted stress-strain model proposed by Mander et al. [5] for confined concrete. This model was originally developed for the confinement effect due to the steel jackets, Eq. (3). This equation has been shown to be applicable to FRP-confined concrete (Spoelstra and Monti [7]). The confining pressure (f_l) for fully wrapped columns, however, must be considered to be linearly variable such that an increase in the strain in the FRP jacket results in a proportional increase in the confining pressure. The confined concrete strength can be computed from Eq. (3) using a confining pressure given in Eq. (4) for fully wrapped columns, that is the result of the maximum effective strain that can be achieved in the FRP jacket as shown in Eqs. (4) through (6).

$$f'_{cc} = f'_c\left[2.25\sqrt{1.0+7.9\frac{f_l}{f'_c}}-2\frac{f_l}{f'_c}-1.25\right] \quad \{\text{ACI440.2R-02}\}(3)$$

$$f_l = \frac{k_a\,\rho_f\,\varepsilon_{fe}\,E_f}{2} \{\text{ACI 440.2R-02}\} \quad (4)$$

$$\rho_f = \frac{2\,n\,f\,t_f\,(b+h)}{bh} \{\text{ACI 440.2R-02}\} \quad (5)$$

$$k_a = 1-\frac{(b-2r)^2+(h-2r)^2}{3bh\,(1-\rho_s)} \quad \{\text{ACI 440.2R-02}\} \quad (6)$$

Where f'_c is the compressive strength of unconfined concrete cylinder, f_l is the lateral confining stress due to wrapping fiber sheets, ε_{fe} is the effective strain induced in FRP reinforcement corresponding to failure (mm/mm), E_f is the modulus of elasticity of FRP (MPa), ρ_f is the FRP reinforcement ratio, and k_a is the efficiency factor which takes into account the geometry of the section (k_a = 1.0 for circular sections).

If the member is subjected to If the member is subjected to combined compression and shear, the effective strain in the FRP jacket should be limited based on the criteria given in Eq. (7).

$$\varepsilon_{fe} = 0.75\,\varepsilon_{fu} \le 0.004 \quad (7)$$

In reality, ACI 440.2R-02 [16] did not report any clear recommendation for prediction of the strength of FRP-confined RC columns under eccentric loading for both circular and rectangular sections. In addition, no requirement was included for evaluation of lateral pressure of partially confined columns.

In the current design guidelines provision (ACI 440.2R-08 [17]), the axial compressive strength of short, normal-weight concrete member confined with an FRP jacket may be calculated using the confined concrete compressive strength, Eq. (8). The main difference between Eq. (8) and Eq. (2) is the factor ψ_f, which is eliminated from Eq. (2).

$$P_n = 0.85\,f'_{cc}\left(A_g - A_s\right) + f_y\,A_s \{\text{ACI 440.2R-08}\}(8)$$

The stress-strain model proposed by Lam and Teng [8, 19] was adopted byACI code [17]. For circular and rectangular sections, this model describes the behavior of FRP-confined concrete subjected to concentric compression load. The factor ψ_f is presented in Eq. (9) to evaluate the maximum confined concrete compressive strength.

$$f'_{cc} = f'_c + 3.30\,\psi_f\,k_a\,f_l \quad \{\text{ACI 440.2R-08}\}\ (9)$$

where,

$$k_a = \frac{A_e}{A_c}\left(\frac{b}{h}\right)^2 \{\text{ACI 440.2R-08}\}(10)$$

$$\frac{A_e}{A_c} = \frac{1-\dfrac{\left[\left(\frac{b}{h}\right)(h-2r_c)^2+\left(\frac{h}{b}\right)(b-2r_c)^2\right]}{3bh}}{(1-\rho_s)} - \rho_s \{\text{ACI 440.2R-08}\}(11)$$

$$f_l = \frac{2E_f\,n\,f\,t_f\,\varepsilon_{fe}}{\sqrt{b^2+h^2}} \{\text{ACI 440.2R-08}\} \quad (12)$$

In Eq. (12), the effective strain level in the FRP at failure ε_{fe} is given by:

$$\varepsilon_{fe} = k_\varepsilon\,\varepsilon_{fu} \quad (13)$$

The FRP strain efficiency factor k_ε takes into account the premature failure of the FRP system. ACI 440.2R-08 [17] recommends that a strain efficiency factor of 0.55 and a minimum confinement ratio f_l / f'_c of 0.08 should be used. Furthermore, the effective strain in the FRP jacket should be limited to the value given in Eq. (14) to ensure the shear integrity of the confined concrete for the members subjected to combined axial compression and bending.

$$\varepsilon_{fe} = 0.004 \le k_\varepsilon\,\varepsilon_{fu} \quad (14)$$

For the purpose of predicting the effect of FRP-confinement on strength enhancement of RC columns under the action of eccentric loading, the current version of ACI guidelines for strengthening concrete

structures with FRPs (ACI440.2R-08 [17]) presents Eqs. (9 -14) for prediction of column strength when eccentricity is less than or equal to 0.1*h*. When the eccentricity is larger than 0.1*h*, the P-M diagram for the FRP-confined member should be constructed using the concrete material properties of the member cross-section under compressive strength. That is to say that P-M diagrams should be developed by satisfying strain compatibility and force equilibrium using the proposed model for stress-strain behavior of FRP-confined concrete. ACI 440.2R-08 [17] assumed a negligible effect for the confining FRP jackets when aspect ratio (*h*/*b*) exceeds 2.0 (limited to 1.5 in ACI 440.2R-02 [16]) or face dimensions *b* or *h* exceeds 900-mm. Based on the recommendations of the early version of ACI guidelines, the enhancement in the strength of the tested columns in this study is insignificant to be considered, which is in contrary to the experimental findings. On the other hand, the approach incorporated by ACI 440.2R-08 [17] to evaluate the enhancement in column strength after wrapping with CFRP sheets can only evaluate the compressive strength of the fully FRP-confined columns. Nonetheless, in case of circular and non-circular sections, both ACI 440.2R-02 [16] and ACI 440.2R-08 [17] guidelines have not introduced any analytical models to predict the strength of RC columns confined with partially-wrapped FRP sheets.

Strength enhancement of the fully-wrapped columns is evaluated using Eqs. (9 -14). Since these equations should be applied for columns subjected to eccentric loading at a distance (*e*) < 0.1*h*, the P-M diagram for the FRP-confined member is constructed for higher eccentricities, as shown in Fig.12. This diagram is developed by satisfying strain compatibility and force equilibrium using Lam and Teng model [8, 19] which was adopted by the ACI 440.2R-08 [17]. Predicted values using Eqs. (9 -14) are superimposed on Fig.12. Also the experimental envelope of P-M diagram is plotted on the same figure for comparison. It is remarkable that the applied Eqs. (9-14) overestimate the effect of eccentricity compared with the P-M diagram constructed based on the same code provisions (ACI 440.2R-08 [17]). However, in general, both Eqs. (9 -14) and P-M diagram underestimate the enhancement in the compressive strength of the tested FRP-confined columns. Compared with the constructed P-M diagram, the error $\left(\frac{P_{n,model}-P_{n,exp}}{P_{n,exp}}\right)$ was around -27% for axially loaded columns, but it increased to -41% and -44% when the applied load is located at eccentricity of 31.5-mm and 41.5-mm, respectively (Fig.12). This underestimation can be attributed to the accuracy of the applied stress-stain model to determine the concrete material properties of the member cross-section. Lam and Teng stress-strain model [8, 19] was based on a few test results of rectangular columns with aspect ratio >1.0. Eight samples were collected by Lam and Teng [19] from which only two samples exhibited enhancement in axial strength capacity. To develop a model with a reasonable accuracy, Lam and Teng [19] tested a new series of fourteen samples; in which, two columns with aspect ratio of 1.5 showed an increase in the axial strength capacity.Despite the well-established accuracy of FRP-confined model proposed by the ACI 440.2R-08 [17] to evaluate the stress-stain behavior for circular sections, it should be focusedin future research for further development to predict the stress-strain behavior of noncircular columns confined with FRP. Also, it is obvious that comprehensive calculations are necessary to construct an accurate P-M diagram, corresponding to compression-controlled failure, to evaluate column strength when eccentricity is larger than 0.1*h*. In the following sections, the effect of partial confinement on evaluation of column compressive strength is considered without any further modification of the stress-strain models.

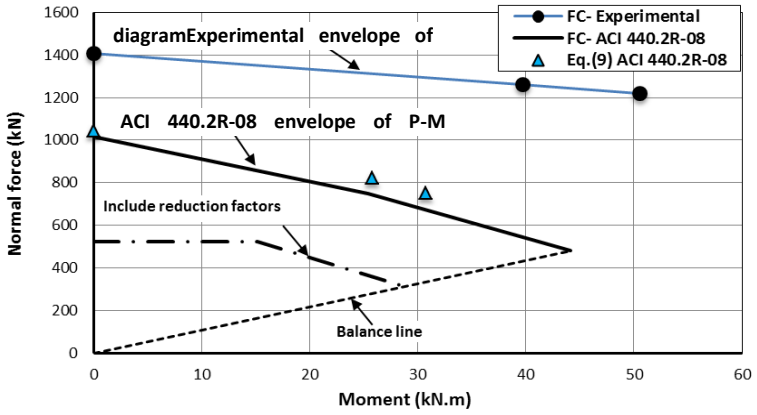

Figure 12.P-M diagram for fully FRP-confined columns using ACI 440.2R-08.

For FRP-confined columns partially wrapped, the efficiency of the wrapping system decreases due to existing of both confined and unconfined zones [6], as shown in Fig.13. In a similar way as circular columns, a modification factor to Eqs. (4) and (12) was introduced to deal with RC rectangular FRP-confined columns which are partially wrapped. Equation (15) identifies the confinement effectiveness coefficient k_p, which takes into account the effectiveness of the hoopstress from the wrapping system on part of the concrete where the confining stress has fully generated as a result of the arch action. The effect of the arch action is proposed as a parabola with an initial inclination of 45^o [6], as shown in Fig.13. Consequently, at the mid-distance between two successive fiber strips, the effectiveconfined concrete area A_e is to be taken into account. So that, the coefficient $k_p$is calculated by considering the ratio (A_e/A_c) [20], where A_c is the area of concrete (= the gross cross-sectional area (A_g)- the area of longitudinal steel (A_s): $A_c = A_g - A_s$).In addition, a definition (ρ_{fp}) is given for the FRP reinforcement ratio of partially confined columns, Eq. (16).

$$k_p = \frac{A_e}{A_c} = \frac{\left(1 - \frac{s}{2(h - 2r_c)}\right)\left(1 - \frac{s}{2(b - 2r_c)}\right)}{1 - \rho_s} < 1.0 \quad (15)$$

$$\rho_f = \frac{2\, n_f\, (b + h)\, b_f\, t_f}{b\, h\, s_f} \quad (16)$$

where b_f is the width of the FRP strips, s_f is spacing between center to center of the CFRP strips (s_f= $b_f$in case of fully wrapping), s (= s_f - b_f) is the clear spacing between two successive wrapped CFRP strips, $\rho_s$is the reinforcement ratio of the longitudinal steel reinforcement with respect to the gross cross-sectional area (= A_s / A_g).

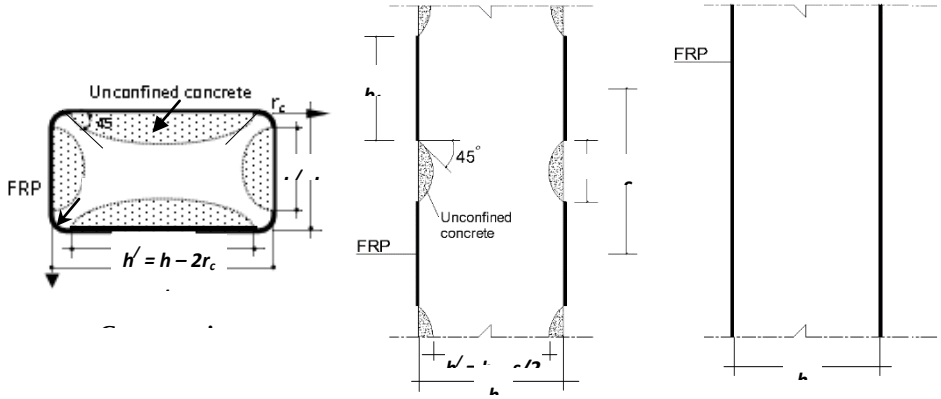

Figure 13. Confining pressure exerted by wrapping FRP sheet on a rectangular column [6]

4.2. Proposed Analytical Modelfor Nominal Compressive Strength of FRP-Confined RC Columns under Eccentric Loading

For columns strengthened with fiber reinforcement jackets and subjected to eccentric loading, the available code provisions have not introduced a direct analytical model for quantitative prediction of the column strength. However, charts or analytical forms are used by engineers as design tools for the evaluation of design strength. This gives a rise to a need for analytical forms to evaluate the design strength of eccentrically loaded columns. Hence, an expression, Eq. (17),is usedto predict the nominal compressive load $P_n$for columnssubjected to loading at eccentricity e_x from column center of gravity: section subjected to combined effect of axial compression P and bending M_x (= $P \times e_x$), as shown in Fig.14. The suggested form is dependent on that the sum of the induced stresses on the column cross-section due to axial force and bending moment (σ_{max}) should be in equilibrium with the maximum compressive strength f'_{cc} of the cross-section after applying the FRP-confinement system. To reflect the impact of mechanical characteristics of the column materials on the evaluated column strength, a modular ratio is defined. For un-cracked section, the modular ratio of elasticity between steel and concrete (n = E_s/E_c: E_c = 4700 $\sqrt{f_c}$ for ACI 318-08 [21]) is used to define both the equivalent column cross-sectional area (A_{eq}) and the second moment of inertia about Y- axis (I_{eq-y}). However, when cracked section is the case, the modular ratio of elasticity $n$should be measured or

approximately taken as 1.5 times that of un-cracked section for normal strength concrete [21].

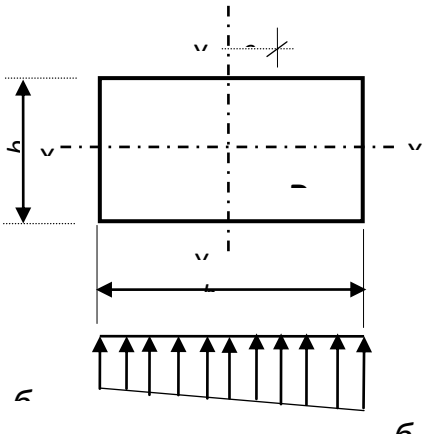

Figure 14. Distribution of normal stresses along the cross-section.

$$\sigma_{max} = P_n \left(\frac{1}{A_{eq}} + \frac{h\, e_x}{2\, I_{eq-y}} \right) = f'_{cc} \quad (17)$$

$$I_{eq-y} = \frac{b\,h^3}{12} + \frac{\pi\, n_s \left[\sqrt{(n-1)}\, d\right]^4}{64} + \sum_{1}^{n_s} (n-1) A_\phi\, x^2 \quad (18)$$

$$A_{eq} = bh + (n-1) A_s \quad (19)$$

where x is the horizontal distancebetween the steel bar and Y-axis, n_s is the number of longitudinal bars, $A_s$and$f_y$are the total areaand yield/proof stress of the longitudinal reinforcement respectively, d and$A_\phi$are the diameter and cross-sectional area of longitudinal bar, respectively, and n is the modular ratio of elasticity between steel and concrete.

It should be clear that the evaluation of the proposed equation depends on the accuracy of the adopted FRP-confined concrete stress-strain model: that is Eq. (17) relies on the value of f'_{cc} . Although the model proposed by ACI 440.2R-08 [17] is in need for further improvement as discussed in the preceding sections, one of the aims of this work to examine validity of the proposed equations to predict the effect of eccentricity on column strength in comparison with the constructed P-M diagram, as shown in Figs.15 and 16. These figures present the constructed P-M diagram for both *FC* and *PC* concrete columns, respectively. The proposed modification for the confinement configuration effect (Eqs. (15 and 16)) was considered in the development of P-M diagrams. These figures show that Eqs. (17-19) can reflect the effect of eccentricity on the column strength with a sound accuracy in regard to the P-M diagrams. But, these equations cannot be further applied when the minimum stress (σ_{min}) in the opposite extreme fiber of the cross-section is tension, as shown in Fig.14. This means that the proposed model is applicable for small eccentricity ratio. Additionally, the compressive strength of the tested columns were predicted using the proposed model, in which f'_{cc} was determined based on stress-strain model of FRP-confined concrete by ACI 440.2R-02 [16]; the results are summarized in Table 3. The proposed modification on the lateral confinement pressure using Eqs. (15 and 16) was considered for the evaluation of partial confinement effect.

Table 3: Evaluation of the proposed model (Eq. 17) using the FRP-confined concretecompressive strength models given by ACI 440.2R-02 (Eq.2) and ACI 440.2R-08 (Eq.8).

Column No.	Experimental P_{max} (kN)	Eq.17 &ACI-02*(Eq.2)		Eq.17 &ACI-08**(Eq.8)	
		P_n (kN)	Error (%)	P_n (kN)	Error (%)
R.0	1124	964	-14	964	-14
R.13	1061	766	-28	766	-28
R.17	1004	690	-31	690	-31
PC.0	1331	1211	-9	1022	-23
PC.17	1118	757	-32	715	-36
FC.0	1406	1315	-7	1029	-27
FC.13	1260	891	-29	816	-35
FC.17	1218	820	-33	722	-41

Note: *ACI-02 means the ACI 440.2R-02; ** ACI-08 means the ACI 440.2R-08; Error = $\left(\frac{P_{n,model} - P_{n,exp}}{P_{n,exp}}\right)$

The combined application of the FRP-confined concrete strength models and the proposed model for the evaluation of column strength shows that Eq. (9) "ACI 440.2R-08 [17]" has inferior effect on the evaluation of column strength than Eq. (3) (ACI 440.2R-02 [16]) for both applied confinement configurations (*FC* and *PC*). For instance, when applying Eq. (9) (ACI 440.2R-08 [17]), the proposed model underestimates the compressive strengths of the concentric loaded columns"*R.0*, *PC.0* and *FC.0*" with values ranged between -14% and -27%. However, for eccentric loaded columns"*R.13*, *R.17*, *PC.17*, *FC.13*&*FC.17*" the errors ranged between -28% and -41% according to the value of eccentricity ratio (e/h): the errors increased as eccentricity ratio increased. On the other hand, when applying Eq. (3) (ACI 440.2R-02 [16]), the proposed model underestimates the compressive strengths of the concentric loaded columns"*R.0*, *PC.0*&*FC.0*" with values ranged between -7% and -14%. However, for eccentric loaded columns"*R.13*, *R.17*, PC.17, *FC.13*&*FC.17*" the errors ranged between -28% and -33% according to the value of eccentricity ratio (e/h): the errors increase as eccentricity ratio increases.

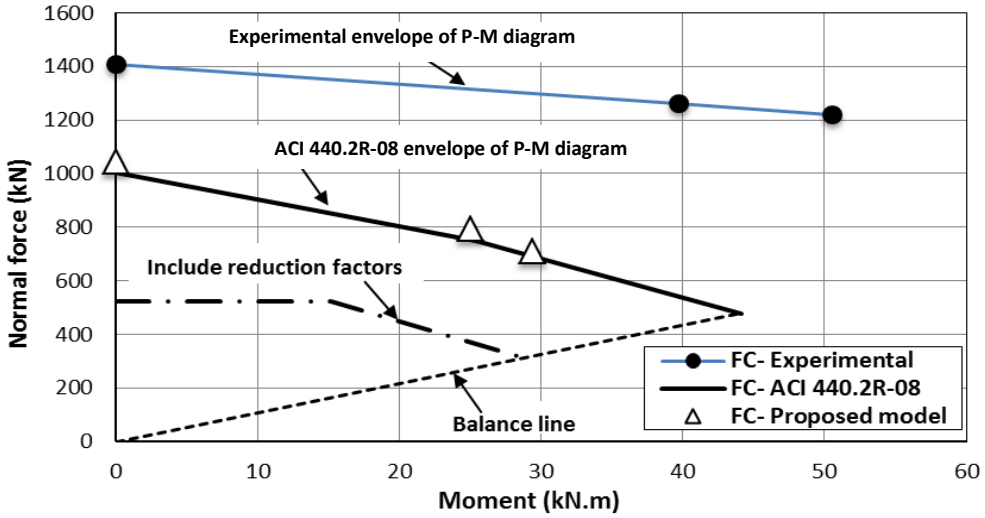

Figure 15. P-M diagram for fully FRP-confined columns using ACI 440.2R-08 in comparison with proposed analytical model.

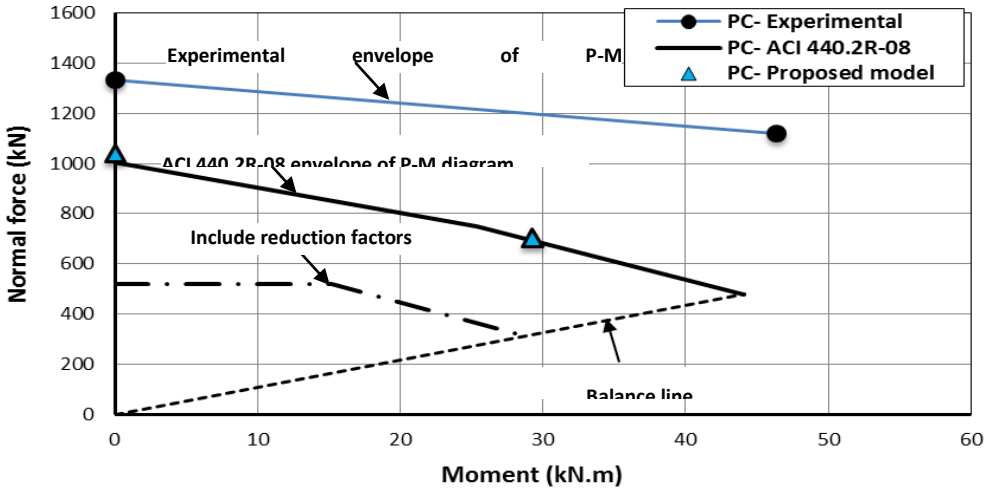

Figure 16.P-M diagram for the partially FRP-confined columns using ACI 440.2R-08 in comparison with proposed analytical model.

The previous discussion demonstrates the proposed model validity in predicting the load carrying capacity of the concentrically loaded columns "un-strengthened and FRP-confined columns", particularly when Eq. (3) (ACI 440.2R-02 [16] is adopted. On the contrary, the validity of proposed model to predict the load carrying capacity of the eccentrically loaded columns needs to be modified and adjusted. Again, the author emphasizes on that a much better estimation of column compressive strength could be obtained when the accuracy of the model in predicting the FRP-confined concrete compressive strength is highly improved.

4.3. Evaluation and Modification of the Proposed Analytical Model

The combined application of the analytical model proposed by the author and both ACI models (ACI 440.2R-02 and ACI 440.2R-08) showed under estimation to predict the strength of FRP-confined RC columns under eccentric loading. However, theproposedanalytical model proved somewhat an acceptable approach to the obtained experimental results when using the modelby ACI 440.2R-02[16] compared with thatwhen using that by ACI 440.2R-08 [17].Such inaccurate prediction is attributed, from the author's point of view, to the fact that the proposed model equates σ_{max} with $f_{cc}^{/}$ regardless the state of loading, eccentric or concentric, see Eqs. (3), (9) and (17).Therefore, modification in the proposed model deals with the adjusted value of the maximum FRP-confined concrete strength under eccentric loading $f_{cc,e}^{/}$should be taken into account when calculating the nominal compressive load P_n of RC columns confined with wrapped FRP sheets.

On the basis of the obtained test results, the concrete strength (maximum stress) under eccentric loading $f_{cc,e}^{/}$ is higher than that under concentric loading $f_{cc,o}^{/}$ (=$f_{cc}^{/}$, see Eq.3). The developed concrete strength depends mainly on the eccentricity ratio *e/h*. Based on the suggested expression (Eq.17) and the obtained experimental load carrying capacity of the different columns and in a contrary manner, the actual confined concrete strength $f_{cc,e}^{/}$ were derived and compared with the predicted confined concrete strength of the corresponding columns subjected to concentric loading $f_{cc,o}^{/}$ (=$f_{cc}^{/}$). In other words, the confined concrete strength of the columns under eccentric loading was calculated in similar way as the corresponding ones under concentric loading. According to the obtained calculations, it was obvious that the obtained $f_{cc,o}^{/}$ is approaching considerably the $f_{cc,e}^{/}$ in case of columns under concentric loading; however, $f_{cc,e}^{/}$ is higher for columns under eccentric loading, particularly for higher *e/h*, see Fig.17. As a result, a modification in predicting $f_{cc,e}^{/}$ should be considered. As the confined concrete strength under eccentric loading depends on various aspects and parameters, for which the influence and interaction are difficult to be quantified analytically, the author proposed a modified relationship among$f_{cc,e}^{/}$,$f_{cc,o}^{/}$, and *e/h*. The modified expression is based on performing a curve fitting which in turn depends on the ($f_{cc,e}^{/}/f_{cc,o}^{/}$) and (*e/h*) data points, see Fig.17 and Eq. (20). So, the FRP-confined concrete strength under eccentric loading $f_{cc,e}^{/}$ may be obtained according to Eq. (20).

$$f_{cc,e} = f_{cc,o}\left(1.0 + 2.10\left(\frac{e}{h}\right)\right) \quad (20)$$

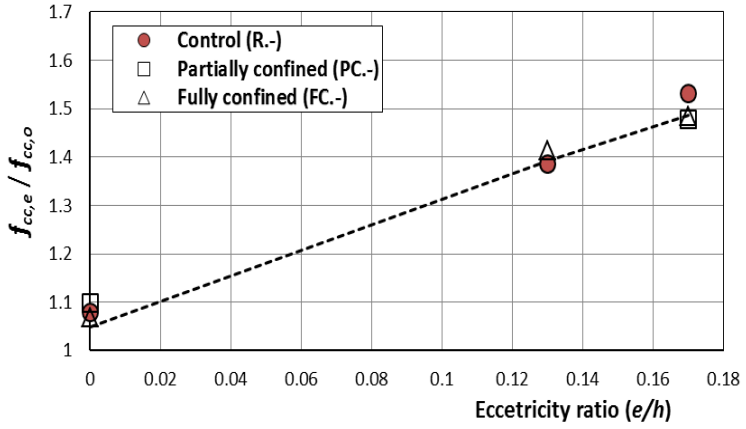

Figure 17. The ratio $f_{cc,e}$ /$f_{cc,o}$ for different eccentricity ratios (*e/h*).

When the above modification was taken into account in calculating the nominal compressive load P_n of RC columns confined with wrapped FRP sheets, the predicted values showed a better estimation and an acceptable approach to the experimental results,

particularly when using ACI 440.2R-02 [16] model, as shown in Table 4. The percentage of errors $\left(\frac{P_{n,model} - P_{n,exp}}{P_{n,exp}}\right)$ranged from -11% to -15% in case of the control columns. However; the percentage of errors ranged from -7% to -10% and from -8% to -9% for fully and partially FRP-confined columns, respectively. What was mentioned before demonstrates well thevalidity of the proposed model in predicting the load carrying capacity of RC FRP-confined columns.

Table 4: Evaluation of the proposed model (Eq. 17) using the FRP-confined concrete compressive strength models given by ACI 440.2R-02 (Eq.2) and the modification $f'_{cc,e}$ (Eq. 20).

Column No.	Experimental P_{max} (kN)	Eq.17 & ACI-02 (Eq.2)		Eq.17, Eq.20 & ACI-02 (Eq.2)	
		P_n (kN)	Error (%)	P_n (kN)	Error (%)
R.0	1124	964	-14	964	-14
R.13	1061	766	-28	903	-15
R.17	1004	690	-31	890	-11
PC.0	1331	1211	-9	1211	-9
PC.17	1118	757	-32	1028	-8
FC.0	1406	1315	-7	1315	-7
FC.13	1260	891	-29	1134	-10
FC.17	1218	820	-33	1113	-9

Conclusions

Based on the conducted experimental study on FRP-wrapped rectangular RC columns under the effect of small eccentricity loading as well as the performed analytical verifications, the following conclusions may be drawn:

1- Confinement of rectangular columns using CFRP sheets is an efficient technique to improve the strength and axial stiffness of RC columns subjected to eccentric loading, particularly in case of fully confinement configuration.

2- The applied strengthening technique enhances bothcracking and maximum loads. The enhancement was higher in case of FC-columns in comparison with their counterparts of PC-columns. However, the value of eccentricity showed inverse effect on bothcracking and maximum loads.

3- A decrease in the ratio of cracking load to maximum load (P_{cr} /P_{max}) was noticed with the increase in eccentricity for the confined columns; however, this is not really detected for the reference columns.

4- The confined columns showed reasonable strains before failure, but the control columns approximately failed at the maximum stress. As a result, the structural ductility of RC columns improved considerably when confined with CFRP sheets, particularly in case of FC-columns. Regardless the confinement configuration, the improvement slightly increases as the eccentricity ratio (e/h) increases.

5- The failure mechanism is affected by the applied FRP-wrapping technique. However, the eccentricity ratio has no influence on the occurred failure mode.

6- Comparison between experimental results of FRP-confined columns with the constructed P-M diagram based on ACI 440.2R-08, the error $\left(\frac{P_{n,model} - P_{n,exp}}{P_{n,exp}}\right)$was around -27% for axially loaded columns, but it increased to -41% and -44% when the applied load is located at eccentricity of 31.5-mm and 41.5-mm, respectively.

7- The authors presents a simple approach (Proposed Analytical Model) that can be applied to find out the effect of FRP-confinement on the compressive strength of concentrically or eccentrically loaded column. This approach depends on the transformed section, considering the linear and nonlinear geometrical properties of the cross-section.

8- The combined application of the analytical model proposed by author and ACI 440.2R-02modelshowed a good estimation to predict the strength of FRP-confined RC columns under eccentric loading, particularly when the modification in the proposed model deals with the adjusted value of the maximum FRP- confined concrete strength under eccentric loading $f'_{cc,e}$is taken into account. The errors $\left(\frac{P_{n,model} - P_{n,exp}}{P_{n,exp}}\right)$ranged from -11% to -15%, from -7% to -10% and from -8% to -9% in case of the control, fully and partially FRP-confined columns respectively.

References

1 SaadatmaneshH,EhsaniMR,andLiMW;StrengthandDuctilityofConcreteColumnsExternallyReinforcedwithFiberCompositesStrips,*ACIStructuralJournal*,Vol.91(4),1994,pp.434–447.

2 MatthysS,TaerweLandAudenaertK;TestsonAxiallyLoadedConcreteColumnsConfinedbyFiberReinforcedPolymerSheetWrapping,*4th InternationalSymposiumonFiberReinforcedPolymerReinforcementforReinforcedConcreteStructures*,31October-5November1999,Baltimore,Maryland,USA,pp.217-228.

3 MirmiranA,ShahawyM,SamaanM,ElEcharyH,MastrapaJCandPicoO;EffectofColumnParametersonFRP-ConfinedConcrete,*ASCEJournalofCompositesforConstructions*,Vol.2(4),1998,pp.175–185.

4 RestrepolJLandDeVinoB;EnhancementoftheAxialLoadCarryingCapacityofR.C.ColumnsbyMeansofFiberglass-EpoxyJackets,*2nd InternationalConferenceonAdvancedCompositeMaterialsinBridgesandStructures*,October1996,Montreal,Quebec,Canada,pp.547-554.

5 ManderJB,PriestlyMJNandParkR;TheoreticalStress-StrainModelforConfinedConcrete,*JournalofStructuralEngineeringASCE*,Vol.114(8),1988,pp.1804–1826.

6 FibBulletin14;FRPasexternallybondedreinforcementofR.C.structures:basisofdesignandsafetyconcept, TG9.3,2001,22p.

7 SpoelstraMRandMontiG;FRP-ConfinedConcreteModel,*JournalofCompositesforConstruction,ASCE*,Vol.3(3),1999,pp.143–150.

8 LamLandTengJ;Design-OrientedStress-StrainModelforFRP-ConfinedConcrete,*ConstructionandBuildingMaterials*,Vol.17,2003a,pp.471-489.

9 LiJandHadiMNS;BehaviorofExternallyConfinedHighStrengthConcreteColumnsUnderEccentricLoading,*Journalofcompositestructures*,62(2)(2003),pp.145–153.

10 HadiMNS;BehaviorofFRPwrappednormalstrengthConcretecolumnsundereccentricloading,*Journalofcompositestructures*,Vol.72(4),April2006,pp.503-511.

11 BoHu,Jian-guoWandGuo-qiangLi;NumericalSimulationandStrengthModelsofFRP-WrappedReinforcedConcreteColumnsUnderEccentricLoading,*ConstructionandBuildingMaterials*,Vol.25(5),May2011,pp.2751-2763.

12 BernátC,LászlóPK;AnalysisofFRPConfinedColumnsUnderEccentricLoading,*Journalofcompositestructures*,Vol.94(3),February2012,pp.1106-1116.

13 *WidiarsaIBRandHadiMNS;*PerformanceofCFRPWrappedSquareReinforcedConcreteColumnsSubjectedtoEccentricLoading,*ProcediaEngineering*,Vol.54,2013,pp.365-376.

14 TomaszT;EffectofEccentricCompressionLoadingontheStrainsofFRCMConfinedConcreteColumns,*ConstructionandBuildingMaterials*,Vol.61,June2014,pp.97-105.

15 ElMaaddawyT;StrengtheningofEccentricallyLoadedReinforcedConcreteColumnswithFiber-ReinforcedPolymerWrappingSystem:ExperimentalInvestigationandAnalyticalModeling,*JournalofCompositesforConstruction2009*;Vol.13,pp.13–24.

16 AmericanConcreteInstitute(ACI)440.2R-02;GuidesfortheDesignandConstructionofExternallyBondedFRPSystemforStrengtheningConcreteStructures",*Rep.No.440.2R-02*,2002,FarmingtonHills,Michigan,USA.

17 AmericanConcreteInstitute(ACI)440.2R-08;GuidesfortheDesignandConstructionofExternallyBondedFRPSystemforStrengtheningConcreteStructures,*Rep.No.440.2R-08*,2008,FarmingtonHills,Michigan,USA.

18 FarghalOAandDiabHMA;PredictionofAxialCompressiveStrengthofReinforcedConcreteCircularShortColumnsConfinedwithCarbonFiberReinforcedPolymerWrappingSheets,*JournalofReinforcedPlasticsandComposites*,Vol.32(19),2013,pp.1406-1418.

19 Lam,L.andTeng,J.;Design-OrientedStress-StrainModelforFRP-ConfinedConcreteinRectangularColumns,*JournalofReinforcedPlasticsandComposites*,Vol.22(13),2003b,pp.1149-1186.

20 FarghalOA; StructuralPerformanceofAxiallyLoadedFRP-ConfinedRectangularConcreteColumnsasAffectedbyCross-SectionAspectRatio,*HBRCJournal*,DOI:10.1016/j.hbrcj.2016.11.002.

21 AmericanConcreteInstitute(ACI)Committee318; BuildingCodeRequirementsforStructuralConcrete(ACI318-68211)andCommentary,2011,FarmingtonHills,MI48331:,2011,Michigan,USA,p.503.

6/11/2018